Title
An inwardly rectifying K+ channel is required for patterning.

Journal
Development (Cambridge, England), 139(19)

ISSN
0950-1991

Authors
Dahal, Giri Raj
Rawson, Joel
Gassaway, Brandon
et al.

Publication Date
2012-10-01

DOI
10.1242/dev.078592

Peer reviewed

Stem cells get cut loose

During tissue maintenance and regeneration, stem cells (SCs) are mobilised and migrate towards sites of tissue turnover or repair. However, owing to the inaccessible nature of most in vivo SC populations, very little is known about the molecular factors that regulate SC mobilisation. Otto Guedelhoefer and Alejandro Sánchez Alvarado tackle this problem by studying SC mobilisation during tissue homeostasis and regeneration in the planarian flatworm *Schmidtea mediterranea* (p. 3510). They show that planarian SCs migrate minimally in the absence of wounding; in partially irradiated animals, SCs do not migrate from the areas that were shielded from radiation to populate irradiated areas. Importantly, the researchers report, amputation increases SC dispersal and induces directional recruitment of SCs to sites of tissue repair, suggesting that factors capable of directing SCs are activated upon amputation. These findings highlight that, in planaria, SC depletion alone is not sufficient to trigger SC migration and that loss of tissue integrity is required to promote the directional migration of SCs.

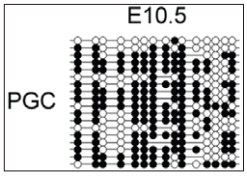

Coupling genome defence to epigenetic reprogramming

DNA methylation plays an important role in gene silencing and repressing transposable elements (TEs). During primordial germ cell (PGC) development, DNA methylation marks are erased during extensive epigenetic reprogramming, so how does this demethylation impact gene expression and TE repression in PGCs? Richard Meehan and co-workers (p. 3623) show that DNA methylation at the promoters of germline-specific genes couples genome-defence mechanisms to epigenetic reprogramming in mouse PGCs. The researchers identify a set of germline-specific genes that are dependent exclusively on promoter DNA methylation for their silencing; their promoters possess specialised chromatin in somatic cells that does not acquire additional repressive histone modifications. This set, they discover, is enriched in genes involved in suppressing TE activity in germ cells, and the expression of these genes is activated during two phases of DNA demethylation in PGCs. These findings suggest that unique reliance on promoter DNA methylation acts as a highly tuned sensor of global DNA demethylation and allows PGCs to be primed to suppress TEs.

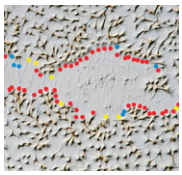

Stan points the way in planar polarity

Many epithelial tissues display planar cell polarity (PCP). This phenomenon has been best studied in *Drosophila* in which most epidermal cells produce hairs at one side that all point in the same direction. The molecular mechanisms underlying PCP establishment remain controversial. Key players are the transmembrane proteins Starry night (Stan; also known as Flamingo), Frizzled (Fz) and Vang Gogh (Vang, also known as Strabismus). Stan, a protocadherin, forms homodimeric bridges between cells. These bridges appear to link Fz and Vang on the abutting distal and proximal faces of adjacent cells, and their resulting asymmetric distributions polarise both cells to point the same way. Now, Struhl, Casal and Lawrence (p. 3665) report the surprising finding that Vang is not essential for cell polarisation. Instead, asymmetric interactions between Stan and Stan/Fz are sufficient to define polarity, and Vang plays an accessory role, probably by enhancing the capacity of Stan to interact with Stan/Fz. These results challenge current models of PCP, although the authors propose an alternative that may reconcile the data.

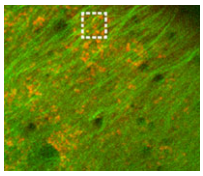

Predicting embryonic axes

In many animals, the polarised transport of maternal factors by the microtubule cytoskeleton is required for setting up embryonic axes. Now, Karuna Sampath and colleagues show that microtubules at the vegetal cortex of early zebrafish embryos are dynamically remodelled and predict the future embryonic axis (p. 3644). Using live imaging, they find that two transient populations of microtubules – perpendicular bundles and parallel arrays – are detected exclusively at the vegetal cortex of fertilised embryos before the first cell division. The perpendicular bundles, which are likely to transport maternal factors via the yolk to the blastoderm, extend from the vegetal cortex and orient along the animal-vegetal axis. The parallel arrays form autonomously even in the absence of sperm entry and fertilisation. Importantly, the asymmetric orientation of parallel arrays shortly after fertilisation predicts where the zebrafish dorsal structures will form. Finally, the authors provide in vivo evidence for cortical rotation-like movements of cytoplasmic granules, similar to those occurring in *Xenopus*, suggesting that such movements might be more common in development than previously thought.

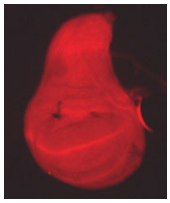

Potassium channels and patterning

Mutations that disrupt the function of the inwardly rectifying Kir2.1 potassium channel cause developmental defects in both humans and mice, but the mechanisms underlying these abnormalities remain unclear. Now, on p. 3653, Emily Bates and co-workers show that disruption of a homologous *Drosophila* potassium channel, Irk2, causes developmental defects by modulating signalling of Decapentaplegic (Dpp), a bone morphogenetic protein (BMP) homologue. The authors find that compromised Irk2 function causes wing patterning defects similar to those observed when Dpp signalling is disrupted. The phenotypes of *Irk2* mutant flies are enhanced by reducing Dpp function. Importantly, the researchers demonstrate that aberrant Irk2 function leads to a decrease in Dpp signalling within the wing: phosphorylation of Mad (a downstream effector of Dpp signalling) and the expression of *spalt* (a transcriptional target of Dpp) are decreased in *Irk2* mutant wing discs. Collectively, these findings identify a novel mechanism by which potassium channels act during development and suggest that BMP pathways might somehow sense alterations in membrane potential.

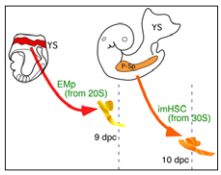

Insights into the origins of HSCs

In mice, haematopoietic stem cells (HSCs) are first found in the dorsal aorta of early embryos shortly after 10.5 days post coitus (dpc) and in the foetal liver at 11 dpc. However, multipotent haematopoietic progenitors can also be detected in the dorsal aorta from 9 dpc. Do these cells contribute to adult haematopoiesis? Here, Ana Cumano and co-workers address this question by characterising this population of cells (p. 3521). The researchers show that multipotent progenitors detected in the dorsal aorta at 9 dpc, which they term immature HSCs (imHSCs), are endowed with long-term reconstitution capacity. Furthermore, they report, these cells are capable of evolving into HSCs under appropriate culture conditions and are able to colonise the mouse foetal liver. Of note, the early colonisation of the foetal liver by imHSCs precedes that of HSCs. Moreover, organ culture experiments suggest that, in the liver environment, imHSCs are able to mature into HSCs, thus identifying a novel stage in HSC development.

Development 139, 3653-3664 (2012) doi:10.1242/dev.078592

An inwardly rectifying K+ channel is required for patterning

Giri Raj Dahal[1,*], Joel Rawson[2,*], Brandon Gassaway[1], Benjamin Kwok[1], Ying Tong[3], Louis J. Ptáček[4,‡] and Emily Bates[1,§]

SUMMARY

Mutations that disrupt function of the human inwardly rectifying potassium channel KIR2.1 are associated with the craniofacial and digital defects of Andersen-Tawil Syndrome, but the contribution of Kir channels to development is undefined. Deletion of mouse *Kir2.1* also causes cleft palate and digital defects. These defects are strikingly similar to phenotypes that result from disrupted TGFβ/BMP signaling. We use *Drosophila melanogaster* to show that a Kir2.1 homolog, Irk2, affects development by disrupting BMP signaling. Phenotypes of *irk2* deficient lines, a mutant *irk2* allele, *irk2* siRNA and expression of a dominant-negative Irk2 subunit (*Irk2DN*) all demonstrate that Irk2 function is necessary for development of the adult wing. Compromised Irk2 function causes wing-patterning defects similar to those found when signaling through a *Drosophila* BMP homolog, Decapentaplegic (Dpp), is disrupted. To determine whether Irk2 plays a role in the Dpp pathway, we generated flies in which both Irk2 and Dpp functions are reduced. *Irk2DN* phenotypes are enhanced by decreased Dpp signaling. In wild-type flies, Dpp signaling can be detected in stripes along the anterior/posterior boundary of the larval imaginal wing disc. Reducing function of Irk2 with siRNA, an *irk2* deletion, or expression of *Irk2DN* reduces the Dpp signal in the wing disc. As Irk channels contribute to Dpp signaling in flies, a similar role for Kir2.1 in BMP signaling may explain the morphological defects of Andersen-Tawil Syndrome and the *Kir2.1* knockout mouse.

KEY WORDS: Inwardly rectifying potassium channel, TGFβ, Dpp, BMP, *Drosophila*, Mouse

INTRODUCTION

Mutations in inwardly rectifying K^+ channels are associated with patterning defects. For example, mutations that disrupt *Kir2.1* are associated with the morphological defects of Andersen-Tawil Syndrome (ATS): cleft palate, micrognathia, hypertelorism, dental abnormalities, clinodactyly, syndactyly and shortened phalanges (Andersen et al., 1971; Tawil et al., 1994; Sansone et al., 1997; Canún et al., 1999; Yoon et al., 2006a; Yoon et al., 2006b). Furthermore, deletion of the mouse *Kir2.1* gene (*Kcnj2* – Mouse Genome Informatics) causes cleft palate and narrow maxilla (Zaritsky et al., 2000).

Inwardly rectifying K^+ channels comprise four subunits (Choe, 2002; MacLean et al., 2002). Mutations that disrupt *Kir2.1* cause periodic paralysis, heart arrhythmia and morphological defects in individuals with ATS. The most severe defects in such individuals are caused by dominant-negative Kir2.1 subunits that complex with other subunits and alter the selectivity filter, affecting K^+ conductivity of the entire heteromeric channels (MacLean et al., 2002; Bichet et al., 2003; McLerie and Lopatin, 2003). The electrophysiological consequences of dysfunctional Kir2.1 are understandable, but the mechanism underlying the developmental abnormalities is unclear.

Despite the growing body of evidence for a role of K+ channels in development, the mechanism by which they influence pattern formation is not understood. Similar cleft palate and digit defects can be caused by loss of transforming growth factor β (TGFβ)/bone morphogenetic protein (BMP), Wnt-Wingless (Wg) or Notch signaling (Jiang et al., 1998; Tucker et al., 1998a; Tucker et al., 1998b; Dudas et al., 2004; Liu et al., 2005; Bandyopadhyay et al., 2006; Casey et al., 2006; Richardson et al., 2009; Xu et al., 2010; Menezes et al., 2010; Ferretti et al., 2011; He et al., 2011; Jin et al., 2011; Lin et al., 2011). We tested the hypothesis that inhibiting Kir2.1 channels interferes with TGFβ/BMP signaling.

The TGFβ/BMP superfamily has orthologous pathways in multicellular organisms (Padgett et al., 1987; Sampath et al.,, 1993; Derynck et al., 1985; Mason et al., 1985; Ohta et al., 1987). In *Drosophila*, Dpp is a BMP homolog that is required for embryonic development, growth and patterning of adult structures, including the wing (Gelbart, 1982; Letsou et al., 1995; O'Connor et al., 2006; Blair, 2007). Dpp binds type 1 and type 2 kinase receptors (Nellen et al., 1994; Letsou et al., 1995; Ruberte et al., 1995). Upon Dpp binding, type 2 receptors phosphorylate type 1 receptors (thickveins), which phosphorylate Mothers against Dpp (Mad) to propagate the signal intracellularly (Kim et al., 1997).

Drosophila is an excellent system for determining the mechanism underlying developmental defects, because conserved developmental signaling pathways are well-defined and non-redundant. Kir2.1 has three homologs in *Drosophila*. Irk2 is 50% identical and 69% similar to Kir2.1. Two other homologs, Irk1 and Irk3, may form heterotetromeric channels with Irk2 as with some Kir channels in mammals. Electrophysiological and expression studies demonstrate that these channels function similarly to mammalian Kir channels (Döring et al., 2002). In this study, we test the hypothesis that Irk2 function is necessary for developmental signaling. We use an *Irk2* dominant-negative allele, *Irk2*-deficient alleles, an *Irk2* p-element allele and RNAi to show that Irk channels are necessary for patterning and growth of the *Drosophila* wing. We conclude that disruption of Irk channels leads to reduction in Dpp signaling and wing defects. These studies explain the mechanism by which K^+ channels regulate development and provide one possible explanation for the defects in individuals with ATS and in *Kir2.1* knockout mice.

[1]Department of Chemistry and Biochemistry, Brigham Young University, Provo, UT 84602, USA. [2]Department of Physiology, University of Texas Health Science Center, San Antonio, TX 78229, USA. [3]Center for Growth, Metabolism and Senescence, College of Life Science, Sichuan University, Chengdu, Sichuan 610064, China. [4]Department of Neurology, University of California, San Francisco School of Medicine, San Francisco, CA 94158, USA.

*These authors contributed equally to this work
‡Present address: Howard Hughes Medical Institute, Chevy Chase, MD 20815, USA
§Author for correspondence (ebates@chem.byu.edu)

Accepted 2 July 2012

MATERIALS AND METHODS

Maintenance of *Drosophila* stocks

Stocks were maintained on cornmeal food at 25°C or 18°C in a Percival incubator model 122 vL (Percival Scientific).

Generation of the *UAS-Irk2DN* and *UAS-Irk2WT* fly strains

irk2A from *Berlin*^{w1118} fly cDNA was cloned into the *Eco*RI and *Xho*I sites of the pUAST vector. PCR was performed with cDNA template and primers (GGAATTCCATGCGTTTCAATTTCTCC and CCGCTCGAGCGGCTAGGAGGCCTGGTCAGA) to add *Eco*RI and *Xho*I sites. Sequencing ensured fidelity of the construct. *UAS-Irk2 DN* was constructed by cutting *irk2A* out of *UAS-irk2 WT* with *Eco*RI and *Xho*I, and ligating into pET. The GYG of *pET-Irk2A* template plasmid was mutated to AAA using a QuikChange Site-Directed Mutagenesis Kit (Stratagene, La Jolla, CA) with the following primers: ACGCAGCACACTATTGCCGCTGCCGTCCGAACCACCTCG and CGAGGTGGTTCGGACGGCAGCGGCAATAGTGTGCTGCGT. *Irk2-DN* was removed from the pET vector with *Eco*RI and *Xho*I restriction enzymes and ligated into pUAST. All constructs were sequenced to verify the GYG to AAA mutations. We injected *UAS-Irk2 WT* or *UAS-Irk2 DN* plasmid with transposase DNA into 1-hour-old *Berlin*^{w1118} embryos. Matured injected flies were crossed to *Berlin*^{w1118} and progeny with the transgene were selected by eye color. *irk1-AAA* and *irk3-AAA* were generated with the same strategy using primer pairs: ACCCAGACGACGATAGCCGCTGCCAATC/CGTCACATAGCGATTGGCAGCGGCTATC (*Irk1-AAA*) and ATCGAGTCCAAGATACGAGTCTACATCATC/GATGATGTAGACTCGTATCTTGGACTCGATGGA (*Irk3-AAA*).

Drosophila strains

The Vienna *Drosophila* RNAi Center (VDRC) provided stocks that express short RNA hairpins complementary to *irk* channel genes under control of an inducible upstream activating sequence (UAS) promoter (Dietzl et al., 2007; Yapici et al., 2008). The GAL4 activator controls expression of genes behind UAS. Ubiquitous expression of GAL4 (and thus the *irk si*RNA or *irkX-AAA* subunits) was achieved with the *daughterless* or *actin* promoter. Wing-directed expression was achieved with MS1096-GAL4 or *engrailed*-GAL4. To accomplish *irk* siRNA, VDRC stocks *irk2* 108140, *irk1* 28430 and *Irk3* 101174 were mated to the flies with appropriate GAL4 driver. The UAS-P35 stock was a gift from Sally Kornbluth (Duke University, NC, USA). All balancer strains, GAL4 driver strains [*MS1096* ($w^{[1118]}$; $P^{\{w[+mW.hs]=GawB\}}$Bx[MS1096]), *engrailed*, *daughterless*, A9 and *actin*], *dpp*^{hr92} and *tkv*^{7} were obtained from the Bloomington *Drosophila* Stock Center.

Generation of *Irk2 Df* strains

An *irk2*-deficient stock [*Df(3R)Irk2exel 6194*$^{\{w[+rC]=xp\text{-}U\}\ exel\ 6194}$] was from the Exelixis custom deficiency generation system (Parks et al., 2004). For clarity, we refer to this strain as *irk2DfA*. The *irk2DfA* deficiency covers 280 kb and removes 25 genes, including *Irk2* and is homozygous lethal. We used the same scheme (Parks et al., 2004) to generate a second *irk2* deficiency. FLP recombinase expression was induced in *Drosophila* larva carrying $P^{(ry+\ t7.2:hsFLP)12}$, $P^{(WH)f002619}$ and $PBac^{(RB)e01487}$ at 37°C in daily 1 hour increments. FLP expression induced recombination between *PiggyBac* $P^{(WH)f002619}$ and $PBac^{(RB)e01487}$ generating flies that lack the genomic region between the two insertion sites, including *irk2* (designated *Irk2DfB*). *irk2DfA/irk2DfB* flies are viable and lack *irk2* entirely without removing more than five surrounding genes. The deletion was verified by PCR.

Irk2 in situ

Standard *irk2* in situ was performed (Lécuyer et al., 2008). The *irk2* probe sequence was: AGGCCTGGTCAGAATGATTGTGGGACAGTTGACGCATGGTAAAGGTGGTTTCTGGTGTGCGGAATCCCTCCTGGATCTTGTAGATCTCGTTCAATTCCCGAGCACTGCACAACGGAGTGTCCACCTGAGTGGTTTCGTTAAAGCGAGCGTAGTCGATTTCATAGGCCTGCAGATCCTTGTTGTACAACACCACTGGATCGAAACGATGTCCCCAAAGGATCTCA.

Quantitative RT-PCR

Total RNA was isolated from third instar larvae (SV Total RNA Isolation System, Promega). Total cDNA was reverse transcribed in vitro using Super Script III reverse transcriptase (Invitrogen, Grand Island, NY). Real-time PCR was accomplished with 100 ng of template cDNA, the Syber Green Assay kit (Applied Biosystems) and 200 nM primers in a Step One plus Real-Time PCR thermal cycling block (Applied Biosystems, Carlsbad, CA). Primer sequences are as follows: RP49, AAGAAGCGCACCAAGCACTTCATC and TCTGTTGTCGATACCCTTGGGCTT; *irk1*, GCCATCGTTTCGTGAATGTGGTGT and AGTGTCCACGTCGTAGGTGTTGTT; *irk2*, ATGGCCGGAATAGTGTTTGCCAA and GGCAAATTACGGCGTGTTTGGAGA; *irk3*, TTATTCTCTGGCCCGATGTGGTGT and GGCAGCATTGAAGAGTTTCGCTGT.

The data were obtained using Step one software V2.1 (Applied Biosystems, Carlsbad, CA). Fold difference was calculated with ΔΔ CT (Livak and Schmittgen, 2001).

Immunohistochemistry and TUNEL staining

Wing discs were isolated from third instar larvae. Discs were stained with anti-phopho-Smad1/5 Ser463/465 (Cell Signaling) (Cao et al., 2006) and 1:250 goat anti-rabbit IgG CY3 (Millipore). Anti-Spalt staining was accomplished with 1:250 anti-Spalt (Halachmi et al., 2007) from Adi Salzberg (Technion-Israel Institute of Technology, Haifa, Israel) and 1:200 goat-anti-rabbit IgG CY3. Achaete was stained with 1:5 mouse-anti-achaete [Developmental Studies Hybridoma Bank (DSHB), Iowa (Skeath and Carroll, 1991)], a 1:200 dilution of the secondary antibody, Alexa Fluor 488 anti-mouse IgG (Invitrogen). Wingless was stained with 1:20 mouse-anti-wingless [DSHB, Iowa (Brook and Cohen, 1996)]. The secondary antibody was 1:200 goat-anti-mouse IgG CY5 (Millipore). Apoptosis was detected using DeadEnd Fluorometric TUNEL (Terminal deoxynucleotidyl transferase dUTP nick end labeling) system (Promega, Madison, WI). Wing discs were mounted with Vectashield mounting medium (Vector Laboratory, Burlingame, CA).

Imaging

Wing discs were imaged at 20× magnification with a Zeiss Axioscope A1 (Carl Zeiss Microscopy LLC, NY) in bright field with a Texas-red filter for anti-pMAD, anti-Spalt and anti-Wingless staining, and a GFP filter for TUNEL and Achaete staining. An AxioCam HRc digital camera with the Axioscope A1 computer program photographed images. For the intensity analysis of anti-pMad staining, control and experimental samples were processed and imaged in parallel with identical settings for exposure (33.2 ms). The fluorescent microscopy images were analyzed with Slidebook (Intelligent Imaging Innovations). Peak intensity was determined by subtracting the minimum fluorescence from the maximum fluorescence intensity in an anterior-to-posterior cross-section of the wing disc. Five independent cross-sections were used for each disc. Anti-Wingless and anti-Achaete stained wing discs were imaged with CY5 and GFP filters, respectively.

Kir2.1 mouse

Generation of the *Kir2.1*-knockout mouse has been described previously (Zaritsky et al., 2000). Bone and cartilage were dissected from newborn pups and placed into 95% ethanol. Ethanol was replaced with 0.03% Alcian Blue, 80% ethanol and 20% acetic acid. Tissue was washed with 95% ethanol before incubation in 2% KOH. Tissue was incubated in 0.03% Alizarin Red. Skeletons were cleared in 20% glycerol. All mouse protocols were approved by the UCSF IACUC.

Statistical analysis

Error bars represent the standard error of the mean (s.e.m.). Raw *P* values were determined using a two-tailed Student's *t*-test. Each experiment consisted of at least three repeated trials. The number of flies tested is given for each figure in the legend.

RESULTS

Kir2.1 mouse phenotypes

Deletion of the gene that encodes Kir2.1 in mice results in patterning defects that are similar to BMP knockout phenotypes. For example, Zaritsky et al. reported that homozygous *Kir2.1* knockout mice have cleft palates (Zaritsky et al., 2000). We further characterized skeletal deformations in homozygous *Kir2.1*

knockout animals (*n*=13) (Fig. 1). The anterior and posterior palatine processes and vomer bones are reduced in size. In addition to the defects that were previously published, we found digit defects in all homozygous *Kir2.1* knockout animals (Fig. 1). It has previously been reported that heterozygous Kir2.1 animals appear normal. However, dissection of heterozygous Kir2.1 mice revealed reduction in the size of anterior and posterior palatine processes and apparent decreased ossification in 98% of heterozygous pups (*n*=40) (Fig. 1C,D). By contrast, no palate or digit defects were found in wild-type siblings (*n*=41). The developmental defects of *Kir2.1* knockout mice are similar to the cleft palate defects of *Tgfb2* and *Tgfb3* knockout animals (Sanford et al., 1997; Taya et al., 1999). Disruption of TGFβ co-factors, regulators and receptors also leads to cleft palate in mice (Peters et al., 1998; Dudas et al., 2004; Bjork et al., 2010). *Kir2.1* knockout digital defects are similar to the BMP2/4 limb conditional knockout (Bandyopadhyay et al., 2006). Other signaling pathways, such as Notch and Wnt, also contribute to these developmental processes (Jiang et al., 1998; Casey et al., 2006; Richardson et al., 2009; Xu et al., 2010). We tested the hypothesis that defective inwardly rectifying K^+ channels interfere with TGFβ/BMP signaling using the genetic tools of *Drosophila melanogaster*. The role of Dpp, a *Drosophila* BMP ligand, is well characterized in the wing (Segal and Gelbart, 1985; Blair, 2007), where *Drosophila* homologs of Kir2.1 are expressed (supplementary material Fig. S1) (MacLean et al., 2002). Thus, *Drosophila* provides an ideal system for investigating whether inwardly rectifying K^+ channel function is necessary for BMP signaling.

Irk2 deficiency disrupts wing patterning

To define the role of Irk2 in development, we examined the phenotypes of flies that lack *irk2* and the surrounding region from 19260K to 19350K of chromosome 3R (supplementary material Fig. S2). *irk2*-deficient flies (*irk2DfA/irk2DfB*) were compared with wild-type flies. When *Irk2DfA*/TM6 is mated to *irk2DfB*/TM6, more than the expected 33% of the progeny are *Irk2DfA/Irk2DfB*, indicating that Irk2 is not necessary for viability (*n*=380). The wings from *irk2*-deficient flies have wing venation defects: incomplete or branched posterior cross veins, incomplete L5 vein, bifurcations of L3 and L4 veins, and wing bristle transformations (Fig. 2; Table 1). Thirty-nine percent of the *irk2*-deficient flies have held-out wings from hinge defects (supplementary material Fig. S3). Rarely, *irk2*-deficient wings are notched or smaller than wild type (Fig. 2C). The penetrance and severity of wing phenotypes in *Irk2*-deficient flies were dependent both on sex and the temperature during development. Phenotypes were most severe in males raised at low temperatures. At 25°C, 38% of male *irk2*-deficient flies had wing defects (*n*=172). Seventeen percent of males that were heterozygous for either *Irk2* deficiency had wing venation defects (*n*=189 and 121). Sixty-two percent of flies harboring a p-element insertion in *irk2* ($Irk2^{G8696}$) had wing venation defects or small wings and 48% had wing hinge defects when raised at 25°C. All male $Irk2^{G8696}$ flies had wing bristle transformations (Fig. 2A,D; supplementary material Fig. S3; Table 1).

To verify that venation defects were the result of *irk2* deficiency, *irk2WT* was expressed ectopically in whole *Irk2*-deficient flies. Wing venation defects other than L5 defects are completely rescued by the ectopic expression of *Irk2WT*. Only 22% of wings of *irk2DfA/irk2DfB; UAS-irk2WT* flies had L5 venation defects compared with 92% of *irk2*-deficient flies that had wing venation defects when raised under the same conditions (Table 1; Fig. 2F).

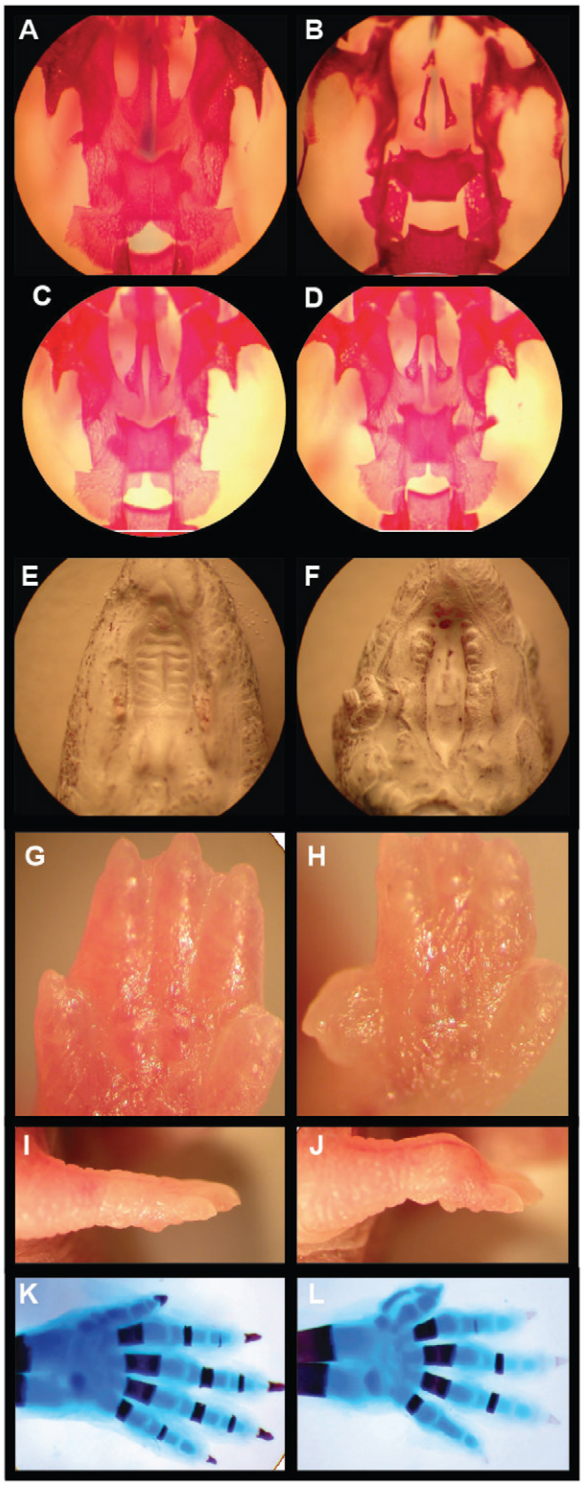

Fig. 1. Knockout of mouse *Kir2.1* causes cleft of the secondary palate and patterning defects of the skeletal digits. (**A-D**) Ventral view of Alizarin Red (bone) staining of palates of newborn wild-type (A), *Kir2.1* knockout (B) and *Kir2.1* heterozygous knockout (C,D) pups. (**E**,**F**) Ventral view of wild-type palate (E) and *Kir2.1* knockout cleft of secondary palate (F). (**G**,**H**) Forelimb of wild-type (G) and *Kir2.1* knockout (H). (**I**,**J**) Ventral view of a wild-type (I) and *Kir2.1* knockout (J) forepaw. (**K**,**L**) Whole-mount forelimb skeletons from newborn animals stained with Alcian Blue and Alizarin Red: wild-type (K); preaxial digit duplication of the forelimb is shown in the *Kir2.1* knockout (L). The dorsal view of the right limb is shown. Anterior is upwards.

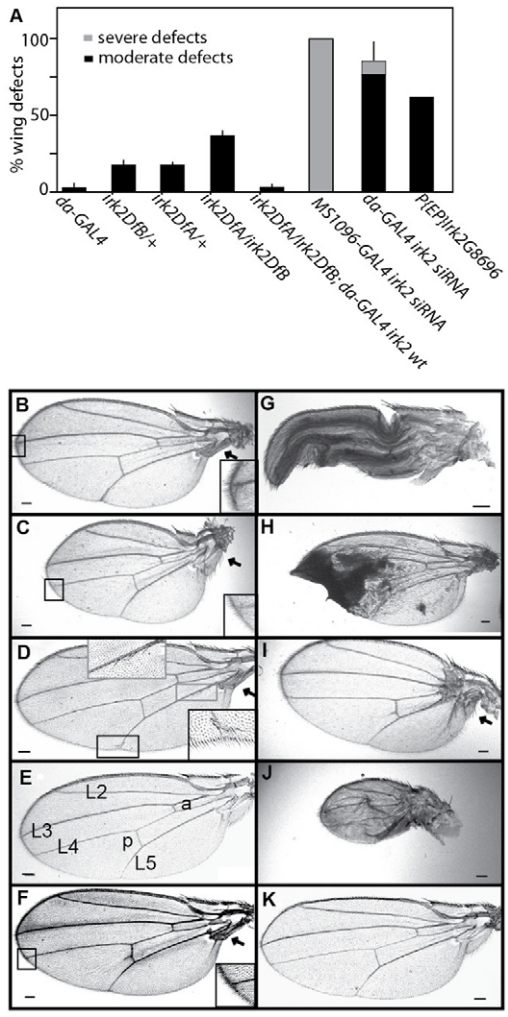

Fig. 2. Reduced *Irk2* function wing phenotypes. (**A**) Quantification of wing defects when *irk2* function is decreased ($n \geq 100$ flies). Error bars indicate s.e.m. (**B**) Bifurcation of L2 and L3 wing veins from *Irk2DfA/Irk2DfB* female. (**C**) Reduced wing size, angled hinge and bifurcation from L4 of *Irk2DfA/Irk2DfB* female. (**D**) Bristle transformations and incomplete L5 from male $irk2^{G8696}$. (**E**) Wild-type male wing L2-5 longitudinal veins; anterior (a) and posterior (p) crossveins are labeled. (**F**) *irk2DfA/irk2DfB* male fly wing. (**G**) Wing expansion defects from *daughterless*-GAL4 *Irk2* siRNA female. (**H**) Ubiquitous expression of *irk2* siRNA causes patches of wing tissue necrosis. (**I**) Small wing and hinge defects from MS1096-GAL4 *Irk2* siRNA female. (**J**) Small wing, hinge and venation defects from MS1096-GAL4 *Irk2* siRNA male. (**K**) Rescued male *irk2DfA/irk2DfB; engrailed-GAL4 UAS-irk2WT* fly wing. Arrows indicate wing hinge defects. Scale bars: 100 μm.

To test for the tissue specificity of the requirement for *Irk2, irk2WT* was expressed using *engrailed-GAL4* in the posterior compartment of *irk2*-deficient wing discs. Wing L5 venation defects were decreased to 37% in flies that express exogenous *irk2WT* in an *irk2*-deficient background. All other *irk2Df/Df* wing defects were rescued by *engrailed*-GAL4; UAS-*Irk2WT* (Fig. 2F,K), indicating that loss of *irk2* function is responsible for wing venation phenotypes and the requirement is partially fulfilled if *irk2* is expressed in the posterior compartment of the wing. As a comparison, only 4% of the male flies harboring the *engrailed-GAL4* driver without the *irk2* transgene had wing venation defects (Table 1). We verified that endogenous *irk2* was deleted and that exogenous *Irk2* was provided in rescued flies by amplifying *irk2* DNA from single flies with primers specific to either genomic *Irk2* or the *UAS-irk2* transgene (Fig. 2). These data show that *irk2* is required non-cell-autonomously in the wing disc to specify wing venation patterning and that the loss of *irk2* is responsible for venation phenotypes that are observed in *irk2*-deficient flies.

Irk2 siRNA expression disrupts wing patterning

To characterize the tissue-specific requirement for *Irk2*, we expressed small-interfering *irk2* RNA (siRNA) under the control of either ubiquitous (*daughterless*) or wing-directed (MS1096) GAL4 drivers. When *irk2* siRNA was expressed ubiquitously using *daughterless-GAL4*, we found defects in 84% of the wings: 73% of the wings had venation defects, 9% failed to expand correctly (Fig. 2G) and 4% of the wings had tissue necrosis (Fig. 2H). Wing-directed expression of *irk2* siRNA causes reduction in wing size, wing venation defects and hinge defects that result in the held-out wings phenotype for all surviving flies (Fig. 2; supplementary material Fig. S3). We designated venation defects and reduction in wing size as moderate defects; any additional defects are designated as severe. Male flies that express *Irk2* siRNA have more severe wing phenotypes than female flies of the same genotype. Ubiquitous expression of *irk2* siRNA can lead to wing expansion defects, whereas wing-directed *irk2* siRNA does not. The difference in phenotypes suggests that expansion of the wing requires Irk function outside the wing whereas patterning requires Irk channel function in the wing disc itself.

Phenotypes that result from ubiquitous or wing-directed expression of the *irk2* siRNA are more severe and more penetrant than phenotypes associated with *irk2* deficiency. We reasoned that expression of *irk2* siRNA could affect the transcription of other *irk* subunits (*irk1* and *irk3*). To determine whether *irk2 si*RNA changed the expression of *irk1* and *irk3*, we used quantitative RT-PCR to quantify *irk1*, *irk2* and *irk3* mRNA from flies that ubiquitously express *Irk2* siRNA and compared mRNA levels with those from flies with the *daughterless-GAL4* driver without the *Irk2* siRNA transgene. *irk2* mRNA is reduced 85.7% in flies that express *irk2* siRNA demonstrating that the *irk2* siRNA effectively reduces

Table 1. Wing venation defects

Genotype	L2	L3	L4	L5	Anterior crossvein	Posterior crossvein
irk2DfB/irk2DfA (n=192)	12%	21%	14%	92%	14%	9%
irk2DfB/irk2DfA engrailed-Gal4 UAS-irk2WT (n=50)	0%	0%	0%	37%	1%	0%
engrailed-Gal4 (n=59)	1%	0%	0%	2.5%	0%	0%
irk2DfB/irk2DfA actin-Gal4-irk2wt (n=81)	0%	0%	0%	22%	0%	0%
actin-Gal4 (n=202)	0%	0%	8%	0%	0%	0%
$Irk2^{G8696}$ (n=107)	2.8%	11%	36%	33%	0	6.5%

Wing venation defects are quantified: in *irk2DfA/irk2DfB*; in the wing-specific rescue flies *engrailed-irk2WT; Irk2DfA/irk2DfB*; in the ubiquitous rescue flies *actin-irk2WT; irk2Df/Irk2Df*; in *engrailed-GAL4* (control); and in $irk2^{G8696}$. All flies represented are male.

expression of *irk2*. Surprisingly, *irk1* was increased 14-fold and *irk3* mRNA levels are increased 4.6-fold in flies that express the *irk2* siRNA (supplementary material Fig. 4A). To determine whether a similar increase in *irk1* and *irk3* expression occurred in *irk2*-deficient flies, we compared *irk1*, *irk2* and *irk3* mRNA levels in wild-type and *irk2*-deficient flies. As expected, no *Irk2* mRNA was detected in *irk2*-deficient flies. *irk3* mRNA levels increased 3.4-fold, but *irk1* transcript levels were not significantly different in *irk2*-deficient flies compared with wild-type flies (supplementary material Fig. S4B). Phenotypes of the *irk2*-deficient wings are less severe than those of *irk2 siRNA*. This leads to the conclusion that Irk subunits are not entirely functionally equivalent. To block the function of the entire Irk channel, we generated a dominant-negative Irk2 subunit.

Expression of dominant-negative Irk2 causes severe wing defects

Inwardly rectifying K^+ channel subunits can form heterotetrameric channels in mammals. Incorporation of a single subunit with a mutated selectivity filter (GYG to AAA) into the complex completely blocks ion flow through the channels in mammals (Bichet et al., 2003). We used the UAS/GAL4 system to express dominant-negative *Irk* transgenes to block the Irk channel in a tissue- and time-specific manner. A transgenic animal expressing this *Irk2* (*Irk2DN*) gene is expected to demonstrate the effects of the loss of the entire channel. By contrast, in an *irk2* null, Irk1 and Irk3 could theoretically form a functional channel without Irk2, thereby at least partially compensating for reduced Irk2 function. We generated three transgenic *Irk2DN* lines: *Irk2DN5.1*, *Irk2DN5.2* and *Irk2DN13*. Ubiquitous expression of *Irk2DN* or *irk2WT* was accomplished by mating transgenic *UAS-irk2WT*/balancer and *UAS-Irk2DN*/balancer flies with *actin-GAL4* or *daughterless-GAL4* transgenic flies. An approximately equal number of transgenic and balancer adult progeny result from the *UAS-irk2WT* cross. No *Irk2DN5.1*- or *Irk2DN5.2*-expressing flies survive from the *UAS-Irk2DN* cross whereas over 90 balancer sibling adults survive. *Irk2DN13*-expressing flies survive to adulthood when raised at 25°C, but only 20% of *Irk2DN13* survive when flies are raised at 18°C (Fig. 3A). Larvae that express *Irk2DN* are marked with *actin*-GFP and can be compared in survival to their balancer siblings after hatching. Only 17% of the larva expected to ubiquitously express *Irk2DN* hatch and none of these survive 48 hours after hatching (Fig. 3B). Endogenous *Irk2* functions in the developing wing, so we directed expression of *Irk2DN* to block Irk channels in the wing disc.

We expressed *Irk2DN* and *irk2WT* in wing discs using *MS1096-GAL4* and *engrailed-GAL4* (Gullaud et al., 2003) to block Irk channels during development. Wing defects include blisters, fusion of longitudinal veins, thickened veins and complete or partial ablation of the wing blade (Fig. 3). Defects were more severe and penetrant in males raised at lower temperatures. To control for sex differences, only female defects are reported in quantification of defects. We report wing defects from two different transgenic lines: *Irk2DN5.1* and *Irk2DN5.2*. Wing-directed expression of *Irk2DN* causes moderate and severe wing defects. Moderate wing defects include wings that are small, collapsed or blistered. Moderate defects also include venation defects such as branching of the posterior cross-vein, L2-3 collapse, L4 bifurcation, incomplete L5 and wing bristle transformations. Severe defects include partial or complete loss of the wing blade.

All of the flies that express *Irk2DN* in transgenic line 5.1 have wing defects with 6% of the wings classified with moderate defects and 94% with severe defects. Expression of *Irk2DN* in transgenic line 5.2

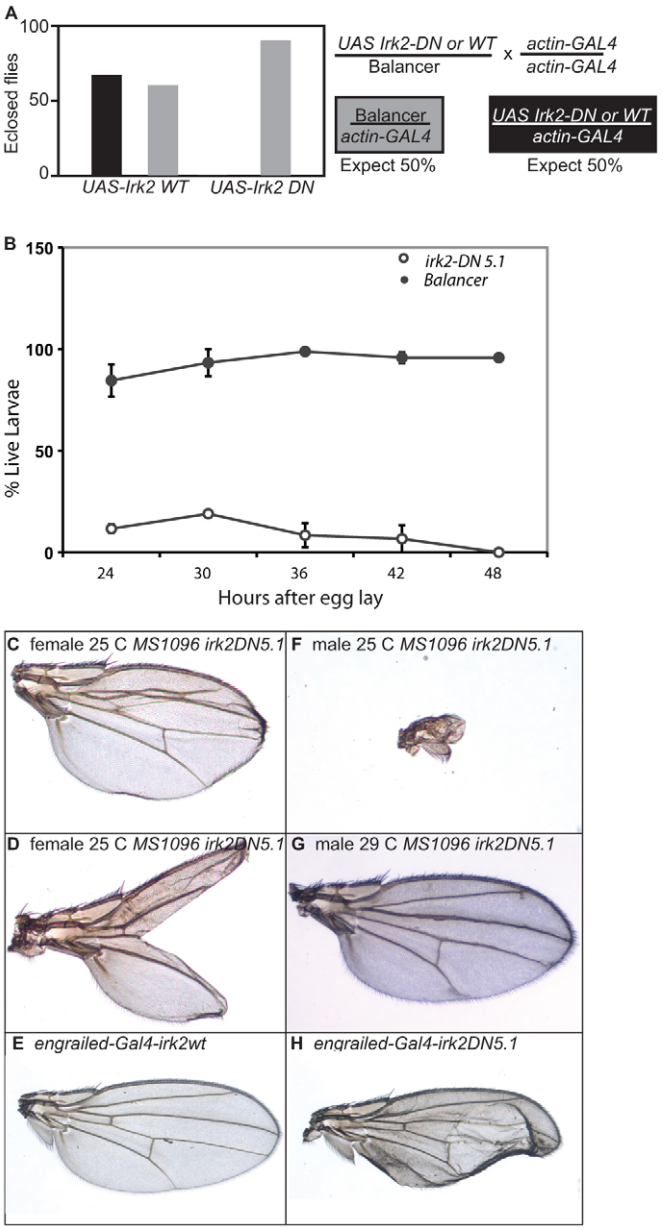

Fig. 3. Phenotypes of flies expressing *Irk2DN*. (**A**,**B**) Graphs of adult (A) and larval (B) survival of *actin-GAL4 UAS-Irk2WT*, *actin-GAL4 UAS-Irk2DN* and siblings without transgene. Error bars indicate s.e.m. (**C**) L2-3 fusion in wing from *MS1096-GAL4 Irk2DN5.1* female at 25°C. (**D**) Bifurcated wing from *MS1096-GAL4 Irk2DN5.1* at 25°C. (**E**) *engrailed*-GAL4 UAS-*irk2WT*. (**F**) Wing of *MS1096-GAL4 Irk2DN5.1* male at 25°C. (**G**) *MS1096*-GAL4 UAS *Irk2DN5.1* at 29°C. (**H**) *engrailed*-GAL4 UAS *Irk2DN5.1* at 25°C.

resulted in 42% moderate wing defects and 4% severe defects (Fig. 3I). Less than 25% of *MS1096-GAL4* UAS-*irk2WT* flies have minor venation defects, similar to *MS1096-GAL4* without a UAS transgene. Expression of *Irk2DN5.2* using the *engrailed-GAL4* driver causes wing venation and blistering defects, whereas expression of *Irk2WT* with the same driver does not cause defects (Fig. 3E,H). As *Irk2DN* expression causes defects that are more severe than loss of *Irk2*, we conclude that Irk2 forms a heteromeric channel that is necessary for patterning of the adult wing in *Drosophila*.

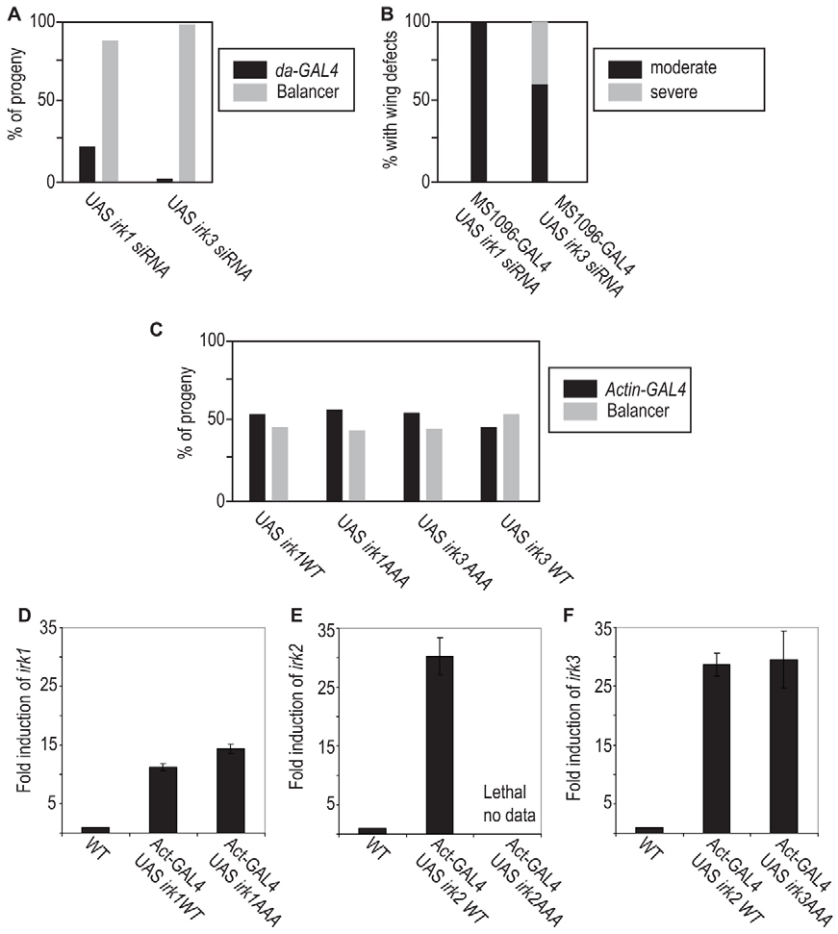

Fig. 4. *Irk1* and *Irk3 siRNA* phenotypes. (**A**) Ubiquitous expression of *Irk1* and *Irk3* siRNA causes lethality. (**B**) Wing-directed *Irk1* and *Irk3* siRNA causes wing venation defects and a reduction in wing size. (**C**) *Irk1-AAA* or *Irk3-AAA* ubiquitous expression does not decrease survival. (**D**) Quantification of *Irk1* mRNA in wild-type, actin-GAL4-UAS *Irk1WT* and actin-GAL4-UAS *Irk1AAA*. (**E**) Quantification of *Irk2* mRNA in wild-type, actin-GAL4-UAS *Irk2WT* and actin-GAL4-UAS *Irk2AAA*. (**F**) Quantification of *Irk3* mRNA in wild-type, *actin*-GAL4-UAS *Irk3WT* and actin-GAL4-UAS *Irk3AAA*. Data are mean±s.e.m.

We reasoned that heteromeric channels could be made up of a combination of Irk1, Irk2 and/or Irk3 subunits. Thus, Irk1 and Irk3 could form a partially functional channel when lacking the Irk2 subunit. If this was the case, we would expect that reduced *irk1* and *irk3* function should cause similar phenotypes to *irk2Df*, *siRNA* or *Irk2DN*. Ubiquitous expression of *irk1* siRNA results in 88% lethality and ubiquitous expression of *irk3* siRNA results in 98% lethality (n=145) (Fig. 4A). As *irk2*-deficient flies survive to adulthood, it is likely that Irk1 and Irk3 play a more substantial role in embryonic development than does Irk2. It is likely that ubiquitous expression of *Irk2DN* causes embryonic lethality by blocking the function of a heteromeric channel that includes Irk1 and/or Irk3.

To examine the contribution of Irk1 and Irk3 to the development of the wing, we expressed *irk1* and *irk3* siRNA in the wing with MS1096-GAL4. Wing-directed expression of *Irk1* and *Irk3* siRNA in the wing results in venation defects in 100% of wings from animals of both genotypes (n=117 and n=92, respectively) (Fig. 4B). Expression of *Irk3* siRNA caused a reduction in wing size and hinge defects in addition to venation defects in 40% of the wings. Wing defects that result from reduced *irk1* and *irk3* support the conclusion that Irk1, Irk2 and Irk3 form a heteromeric channel that is necessary for wing development.

To determine if the conserved GYG of Irk1 and Irk3 play the same structural role as for Irk2, we generated mutant alleles of both, changing the conserved GYG to AAA. Ubiquitous expression of *irk1-AAA*, *irk1WT*, *irk3-AAA* or *irk3WT* did not decrease survival or cause wing defects (n=127 *Irk1-AAA*, 129 *Irk1WT*, 132 *Irk3-AAA* and 124 *Irk3WT*) nor did wing-directed expression of mutant irk1-AAA or irk3-AAA cause wing defects (n=107 and 113) (Fig. 4C). We ensured that the *Irk2DN* and *Irk2WT* constructs were expressed using QRT-PCR (n=3 trials) (Fig. 4D-F). We conclude that Irk1, Irk2 and Irk3 are important to channel function, but play different structural roles in the heteromeric Irk channel.

Reduced Dpp signaling enhances *Irk2DN* phenotypes

Disruption of *irk2* function with siRNA, *irk2* deficiency or expression of *Irk2DN* causes defects in the wing that are similar to defects caused by compromised Dpp signaling (Gelbart, 1982; Spencer et al., 1982; Irish and Gelbart, 1987; Letsou et al., 1995; Cook et al., 2004; del Alamo Rodríguez et al., 2004). A possible explanation for *Irk2* developmental defects is that Irk channels are necessary for proper Dpp signaling. We undertook genetic interaction studies by disrupting the function of Dpp (BMP ligand) or Thickveins (Tkv, BMP type 1 receptor) in an *Irk2DN* background.

To determine how defective Dpp signaling affects the *Irk2DN* wing phenotype, either the *Irk2DN* or the *irk2WT* transgene was expressed in wings of dpp^{hr92}/+ or tkv^{7}/+ flies. Owing to differences in phenotype severity, we report defects from females only. Defective Dpp signaling enhances *Irk2DN* phenotypes (Fig. 5). When *Irk2DN5.2* is expressed in a tkv^{7}/+ mutant background, total wing defects increased from 46% to 72%. When *Irk-2DN5.2* is expressed in a dpp^{hr92}/+ background, 84% of flies have wing defects and 29% are severely defective, whereas without compromised Dpp signaling, only 4% are classified as severe in the

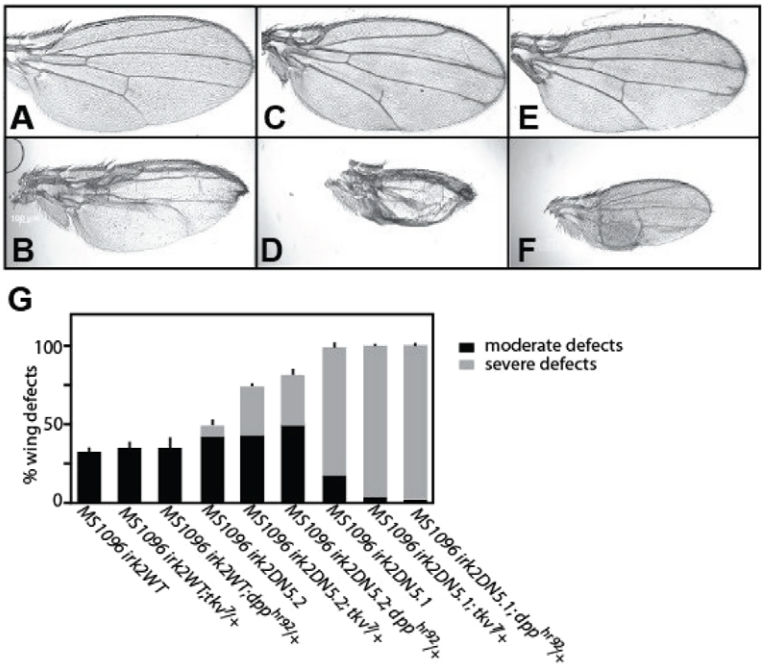

Fig. 5. Reduced Dpp or Thickveins function enhances *Irk2DN* phenotypes. (**A**,**B**) *Irk2DN5.2* female incomplete L5. (**C**) Thickened, bifurcated veins of dpp^{hr92}/+ female wing. (**D**) *Irk2DN5.2/+;* dpp^{hr92}/+ female wing is small and missing veins. (**E**) Thickened, bifurcated L2, L3 and L4 veins, and incomplete anterior crossvein of tkv^{7}/+ female wing. (**F**) *Irk2DN5.2/+;* tkv^{7}/+ female wing is small and missing veins. (**G**) Quantification of wing defects of *MS1096-GAL4 UAS-irk2WT*, *UAS-Irk2DN5.1*, *UAS-Irk2DN 5.2* and with dpp^{hr92}/+ or tkv^{7}/+. *n*>100 for all genotypes. Data are mean±s.e.m.

Irk2DN5.2 line (Fig. 5). In the more severe *Irk2DN5.1* transgenic line, 94% of flies have severe wing defects and when *Irk2DN5.1* is expressed in a tkv^{7}/+ background, 99% of the flies have severe wing defects. Similarly, 97% of flies have severe wing defects in *Irk2DN5.1;* dpp^{hr92}/+ flies. Expression of the wild-type *Irk2* transgene caused minor wing venation defects in 20% of the flies, but these defects did not increase in penetrance or severity when the transgene was expressed in the dpp^{hr92}/+ or tkv^{7}/+ background (16% and 15%, respectively). Thus, *Irk2DN* phenotypes are enhanced by reducing function of Dpp or its type 1 receptor, Tkv.

Dpp signaling is disrupted by aberrant Irk2 function

Enhancement of *Irk2DN* phenotypes by reduced Dpp or Tkv function suggests that Dpp signaling is compromised in flies with defective Irk channel function. To explore this possibility, we looked at Dpp signaling in the larval wing imaginal disc, a precursor to the adult wing. Dpp-bound Tkv phosphorylates the C-terminal of Mothers against Dpp (Mad) in two stripes that form the border between the anterior and posterior compartments of the wing disc (Teleman and Cohen, 2000). To determine whether Dpp

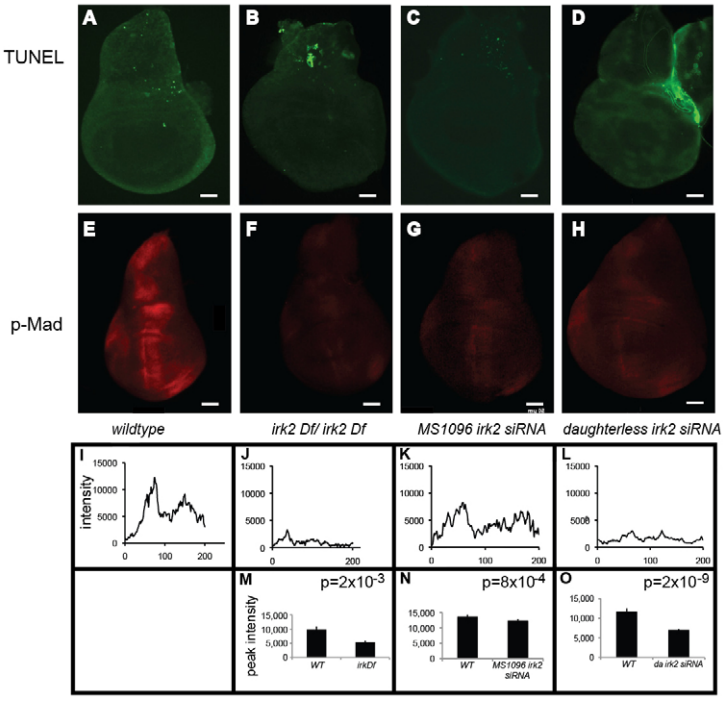

Fig. 6. Reduced Mad phosphorylation in *Irk2DfA/Irk2DfB* and *Irk2* siRNA wing discs. (**A-D**) TUNEL-stained wing discs. Anterior is rightwards. (**E-H**) Anti-p-Mad stained wing discs. (**I-L**) Relative fluorescence intensity across a posterior to anterior cross-section of the anti-p-Mad-stained wing disc shown in E-H. (**M-O**) Graphs of average peak intensity of control and *irk2DfA/irk2DfB* (M), control and MS1096-GAL4 *irk2 siRNA* (N), and control and *daughterless-GAL4 Irk2 siRNA* (O). Control and experimental discs were stained and imaged in parallel. Graphs represent average peak intensities for *n*>7 anti-p-Mad-stained discs. Peak intensity is determined by subtracting minimum from maximum fluorescence intensity in a posterior to anterior cross-section of the anti-p-Mad stained wing disc. Data are mean±s.e.m. Scale bars: 50 μm.

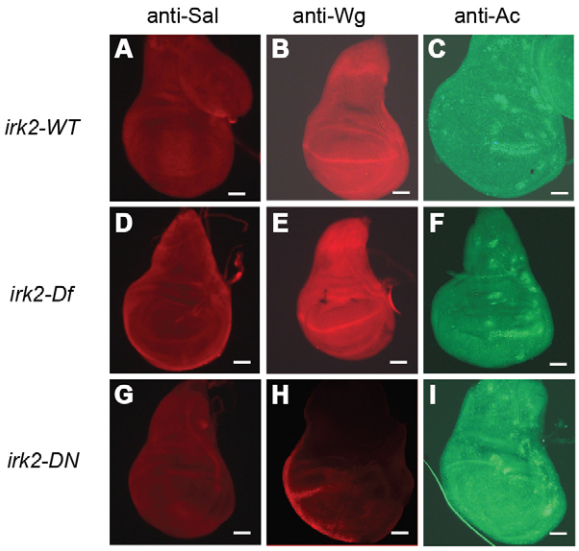

Fig. 7. Immunohistochemistry demonstrates that Dpp signaling is reduced in *Irk2DN* and *Irk2DfA/Irk2DfB*. (**A-I**) Wild-type wing discs (A-C), *irk2DfA/irk2DfB* (D,E) and *Irk2DN5.1* (G-I) stained with anti-Spalt (A,D,G), anti-Wingless (B,E,H) and anti-Achaete (C,F,I). Scale bars: 50 μm.

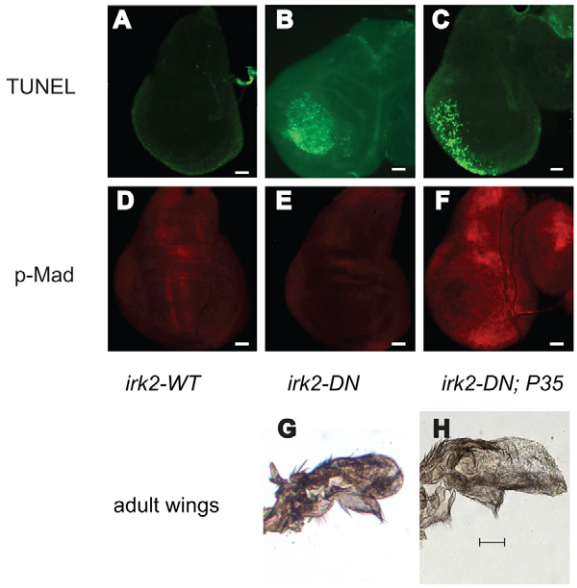

Fig. 8. Irk2DN expression causes apoptosis and eliminates p-Mad staining in the third instar larval imaginal wing disc. (**A-C**) TUNEL stained wing disc. (**D-F**) Anti-p-Mad stained wing disc. (A,D) *MS1096-GAL4-Irk2WT.* (B,E) MS1096-GAL4-*Irk2DN.* (C,F) *MS1096-GAL4-UAS-Irk2DN; P35*. *n*>10 discs. (**G**) *MS1096-GAL4-UAS-Irk2DN; P35* male wing. (**H**) Control *MS1096-GAL4-UAS-Irk2DN* male wing. Scale bars: 50 μm.

signaling is interrupted by disruption of *irk2* function, we used an antibody to measure phosphorylation of the C-terminal site of Mad (p-Mad). Two stripes of p-Mad are intact in *Irk2* deficient and *Irk2* siRNA-expressing wing discs, but the stripe intensity is lessened compared with wild type (Fig. 6). TUNEL staining shows that reducing function of *irk2* does not cause apoptosis, and therefore is not the cause of decreased p-Mad (Fig. 6). Spalt (Sal), a transcriptional target of Dpp, was reduced in *irk2-DfA/irk2-DfB* wing discs and was not detectable in *Irk2DN*-expressing wing discs, supporting the conclusion that Dpp signaling is disrupted by blocking Irk channels (Fig. 7). By contrast, patterns of two genes that are not regulated by Dpp, *wingless* and *achaete*, are intact in *irk2*-deficient wing discs (Fig. 7).

Expression of *Irk2DN* causes the most severe wing phenotypes and is predicted to block the Irk channel completely. We found that when MS1096-Gal4 drives expression of *Irk2DN*, phosphorylation of Mad is completely blocked in the anterior/posterior boundary of wing pouch (Fig. 8A-C). p-Mad staining was intact when flies expressed the *irk2WT* transgene. Irk2DN expressed by other wing-directed Gal4 drivers (Marquez et al., 2001), *en-Gal4;Irk2DN5.1*, *A9-Gal4;Irk2-DN13* and *A9-Gal4;Irk2-DN5.1*, also profoundly decreases p-Mad staining and can decrease the size of the wing disc (supplementary material Fig. S5). Less that 5% of *en-Gal4; Irk2-DN5.1* and *A9;Gal4-DN5.1* flies survive past early larval stage.

MS1096-Gal4;UAS*Irk2DN5.1* wing discs are fragile and thinned in the wing pouch region that becomes the wing blade and hinge. TUNEL staining shows that apoptosis occurs in the wing pouch of MS1096-Gal4;UAS*Irk2DN* wing discs. Very little apoptosis is detected in the wing discs of flies expressing *irk2WT* (Fig. 8). In *Irk2DN*-expressing wing discs, *wingless* and *achaete* patterns are normal surrounding the region that dies via apoptosis (Fig. 7).

Disruption of the K+ current with Irk2DN causes complete loss of the two stripes of p-Mad that form the proximal-distal axis of the wing disc and also causes apoptosis of many of the cells that are under the influence of the Dpp signal. At least two possibilities explain these phenotypes. First, as Dpp protects against apoptosis in the wing (Letsou et al., 1995; Adachi-Yamada et al., 1999; Adachi-Yamada and O'Connor, 2002; Moreno et al., 2002; O'Connor et al., 2006; Ziv et al., 2009), blocking the K^+ current could interfere with Dpp signaling, leading to apoptosis and wing defects. Alternatively, blocking Irk could directly cause apoptosis, leading to reduced Dpp signaling. To test which of these possibilities explains *Irk2DN* wing defects, we blocked apoptosis in cells of the wing discs that express *Irk2DN* and asked whether Dpp signaling occurs and whether the wing defects are rescued. Exogenous expression of P35 blocks caspase activity, preventing apoptosis (Hay et al., 1994). TUNEL staining confirmed that apoptosis does not occur in the wing pouch cells that express both *Irk2DN* and P35 (Fig. 8). Wing pouch cells give rise to the wing blade. The severe wing phenotypes of *MS1096-GAL4-Irk2DN;P35* are indistinguishable from those of wings that express only *Irk2DN* (Fig. 8). As blocking apoptosis in the wing pouch does not rescue the wing phenotype, we conclude that apoptosis is fully responsible for wing blade defects. Apoptosis occurs in periphery of the wing disc, but not in the center where both P35 and Irk2DN are expressed. Therefore, Irk2DN does not cause apoptosis cell-autonomously, but could cause apoptosis of peripheral cells by compromising a Dpp gradient (Adachi-Yamada et al., 1999). Together, these data suggest that Dpp signaling is disrupted by *Irk2DN*, which leads to apoptosis and *Irk2DN* wing defects.

DISCUSSION

The morphological defects associated with ATS suggest that Kir2.1 function is necessary for human development. We and others have shown that these defects are recapitulated in a mouse knockout of Kir2.1 (Zaritsky et al., 2000). Here, we show that reducing function

of the Irk2 ion channel causes developmental defects in *Drosophila*, probably by disrupting Dpp signaling. Four points support this conclusion. First, mouse and fly Kir2.1/*Irk2* phenotypes are similar to TGFβ/BMP mutant phenotypes. Second, reduced Dpp signaling enhances *Irk2DN* phenotypes. Third, phosphorylation of Mad and *spalt* expression are decreased in mutant *Irk2* wing discs. Last, Irk2DN induces apoptosis of cells within the region of Dpp influence, but outside the region of *Irk2DN;P35* expression.

Our data show that the *Drosophila* Irk channel is heteromeric. Loss of any Irk subunit alone causes minor defects compared with severe defects caused by an *Irk2DN* subunit predicted to block the channel. This suggests that, in the absence of one Irk subunit, the others partially compensate.

Irk2 phenotypes are more severe and penetrant when flies develop at colder temperatures, regardless of the mechanism by which *Irk2* function is reduced: transgenic *Irk2DN* expression, *irk2* deletion, p-element insertion or *irk2* siRNA expression. We observed this temperature effect for three independent *Irk2DN* transgenic lines under the control of many different GAL4 drivers. Although the GAL4 system generally increases transgene expression at higher temperatures, *Irk2DN* phenotypes are most severe at 18°C, less severe at 25°C and least severe at 29°C. This suggests that the process by which Irk channels contribute to signaling is dependent on temperature.

Irk2 phenotypes are reminiscent of mutant *dpp*, *tkv* and *punt* wing phenotypes (Letsou et al., 1995; Zecca et al., 1995; de Celis, 1997; Adachi-Yamada et al., 1999). The L2-3 and L4-5 collapse and loss of the majority of the wing blade are similar to mutant *dpp* or its target, optomotor-blind (*omb*) (Cook et al., 2004; del Alamo Rodríguez et al., 2004; Tabata and Kornberg, 1994). *irk2*-deficient flies, mutant *irk2* and *irk2 siRNA* flies have similar hinge phenotypes to those caused by mutant *dpp* alleles (Gelbart, 1982; Spencer et al., 1982; Irish and Gelbart, 1987). Furthermore, *Irk2DN* phenotypes are enhanced by reducing function of Dpp or its receptor. Together, these data suggest that *irk2* wing phenotypes can be explained by disruption of Dpp signaling.

Reducing function of *irk2* by deletion, siRNA or *Irk2DN* reduces p-Mad in the wing disc. We confirmed that loss of *irk2* reduces Dpp signaling by measuring decreased levels of Spalt, a p-Mad transcriptional target. Activation of the Wg pathway negatively regulates Dpp signaling by reducing perdurance of p-Mad, presenting the possibility Wg is affected by Irk2 (Eivers et al., 2009a; Eivers et al., 2009b; Eivers et al., 2011). Expression of both *wingless* and *acheaete* are normal in *irk2*-deficient wing discs and outside the region where cells have died via apoptosis in *Irk2DN*-expressing wing discs. However, we have not ruled out the possibility that Wingless or other developmental pathways are also affected by Irk channel function.

We find that blocking apoptosis in the cells that express *Irk2DN* does not rescue the associated wing phenotypes. A wing can develop with normal size and patterning after x-irradiation-induced apoptosis of half of the wing disc cells during development (Hay et al., 1994; Huh et al., 2004; Martín et al., 2004; Pérez-Garijo et al., 2004; Ryoo et al., 2004). Dpp signaling is responsible for compensation for the lost apoptotic cells and preservation of patterning in damaged wing discs (Pérez-Garijo et al., 2005). The failure of Irk2DN;P35-expressing discs to compensate for apoptotic cells supports the hypothesis that Dpp signaling is disrupted in tissues that express *Irk2DN*.

How could Irk2 affect Dpp signaling? It could be that maintenance of membrane potential is important for the production, distribution or propagation of the Dpp signal. Alternatively, there may be communication between Irk channels and the Dpp signaling cascade upstream of Mad activation. Distribution and propagation of Dpp and other BMP/TGFβ signals are aided by the heparan sulfate proteoglycans (HSPGs) (Jackson et al., 1997; Grisaru et al., 2001; Paine-Saunders et al., 2002; Fujise et al., 2003). Changes in sodium concentrations inhibit sulfation of heparan sulfate and reduce the sensitivity of cells to FGF. It is interesting to speculate that a change in local K^+ concentrations could interfere with HSPGs, receptor localization, stabilization of the receptor complex, phosphorylation events or production or distribution of the Dpp ligand (Fig. 9). It is also possible that Mad requires K^+ for recruitment to the membrane as actin requires Ca^{2+} for that purpose (Lu et al., 2011). We have not directly established whether Irk2 is required cell-autonomously, but we favor the model that Irk2 function is required for Dpp signaling events outside the cell rather than for intracellular phosphorylation for two reasons. First, *en*-GAL4 expresses UAS-*irk2WT* in the posterior compartment of the wing disc, but rescues *irk2* deficient phenotypes in the whole wing. Second, when *Irk2DN* and P35 are expressed together, apoptosis occurs well outside of the region of MS1096 expression, consistent with morphogen causation.

If inwardly rectifying K^+ channels are necessary for Dpp signaling to designate wing patterning, how could Irk subunits have been missed in Dpp modifier screens? The partial redundancy of the Irk subunits make severe phenotypes unlikely unless all of the subunits are compromised. Phenotypes are not severe at 25°C, the temperature at which development occurs for most screens. Third, the necessity of Irk2 seems to be tissue specific. Dpp is required for patterning of multiple structures, but in screening multiple GAL4 drivers, expression of *Irk2DN* causes defects in only a few of these.

Many BMP/TGFβ-dependent processes go awry when Kir2.1 is not functional in humans and in mice. The phenotypes of Kir2.1 knockout mice are reminiscent of the morphological defects of ATS: cleft palate, incomplete dentition and digit abnormalities. All of these phenotypes have also been associated with defects in TGFβ superfamily signaling. For example, TGFβ2 and TGFβ3 knockout animals have cleft palate (Sanford et al., 1997; Taya et al., 1999). Loss of BMP4 impedes proper tooth development (Neubüser et al., 1997; Jernvall et al., 1998; Tucker et al., 1998a; Tucker et al., 1998b). Deletion of Pax9, which activates BMP4 transcription, causes cleft palate, incomplete dentition, and extra digits in mice (Peters et al., 1998). A conditional knockout of BMP2 and BMP4 in the forepaw causes extra digits like the *Kir2.1* knockout (Bandyopadhyay et al., 2006). BMP signaling is responsible for inhibiting growth of extra digits and initiating apoptosis to separate digits in mice (Schaller et al., 2001; Schaller and Muneoka, 2001; Zuzarte-Luis and Hurle, 2005). Although the developmental defects associated with *Kir2.1* knockout are incompletely characterized in the mouse, these BMP-like phenotypes support the hypothesis that disruption of *Kir2.1* interferes with TGFβ/BMP signaling in mammals.

The finding that inwardly rectifying K^+ channels are necessary for BMP signaling in the *Drosophila* wing alters the landscape of current research by demonstrating that K^+ channels contribute significantly to development. How broadly can these findings be applied to other K^+ channels? A gain-of-function GYG to SYG change in the selectivity filter of the G protein-coupled Irk2 (GIRK2) channel allows it to pass Na^+ and Ca^{2+}, which alters cerebellar development in the weaver mouse (Rakic and Sidman,

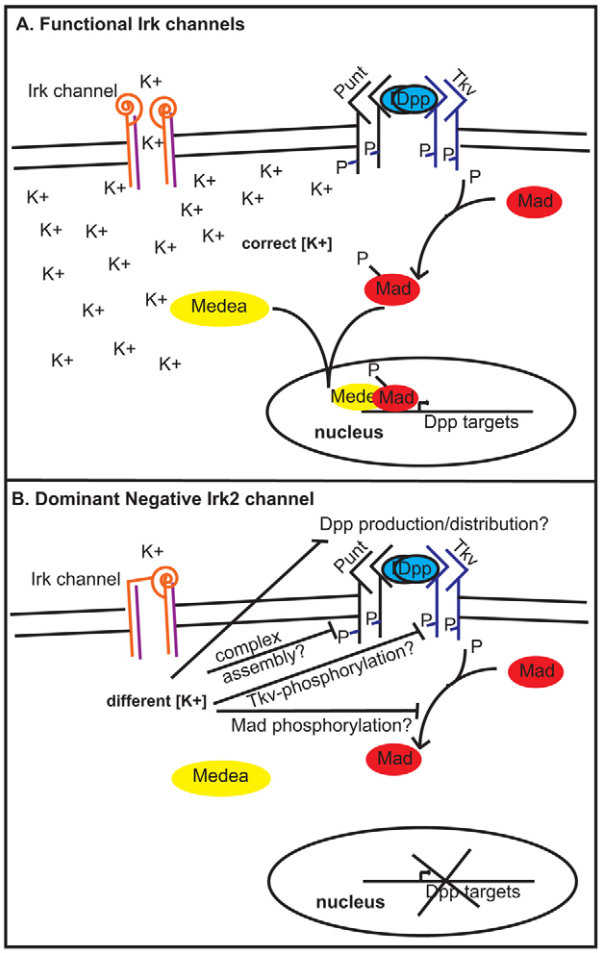

Fig. 9. Model for Irk channels in Dpp signaling. (**A**) With functional Irk channels, Dpp binds type 1 (Thickveins) and type 2 (Punt) kinase receptors that are stabilized by proteoglycans (Dally, not shown). Upon Dpp binding, activated type 1 receptors phosphorylate Mad. P-Mad binds Medea and enters the nucleus to affect transcription. (**B**) Blocking Irk channels hinders Mad phosphorylation. Irk channels could be necessary for Dpp production/distribution, receptor complex stabilization or Tkv/Mad phosphorylation.

1973; Hatten et al., 1984; Hatten et al., 1986; Patil et al., 1995; Silverman et al., 1996; Tong et al., 1996). However, deletion of GIRK2 allows mice to develop normally (Signorini et al., 1997). Therefore, developmental defects of weaver mice are presumed to be due to changes in Na^+ and Ca^{2+}, rather than changes in K^+, levels. By contrast, the mutations that are associated with ATS cause loss of Kir2.1 function (Bendahhou et al., 2003; Hibino et al., 2010) and the *Kir2.1* knockout mouse has severe developmental defects. Our data presents a rationale for inquiry into the putative contribution of other K^+ channels to developmental signaling.

Altering Irk channels interferes with BMP signaling to contribute to morphological abnormalities in *Drosophila*. It is likely that the developmental defects associated with ATS and the *Kir2.1* knockout mouse are similarly due to defective TGFβ/BMP signaling. If Kir2.1 channel function is necessary for TGFβ/BMP signaling in mammals, the Kir channels could represent new potential therapeutic targets for slowing tumor growth and metastasis.

Acknowledgements
We thank Dr Allen Buskirk, Dr Anthea Letsou, and Drs Peter and Alex Bates for editing. We thank the Bloomington *Drosophila* Stock Center, the Vienna *Drosophila* Stock Center, Dr Anthea Letsou and Dr Sally Kornbluth for fly stocks. We also thank Adi Salzberg for anti-Spalt. We thank Ree Lu, Phoebe Lin, Devon Kinghorn, Alex Johnson, Elise Wilson and Abigail Gehrett for wing disc dissections.

Funding
This work was funded by the Howard Hughes Medical Institute, the Muscular Dystrophy Association and the Sandler Neurogenetics Fund (to L.J.P.), and by the Brigham Young University Cancer Research Center (to E.A.B. and G.D.). Deposited in PMC for release after 6 months.

Competing interests statement
The authors declare no competing financial interests.

Supplementary material
Supplementary material available online at
http://dev.biologists.org/lookup/suppl/doi:10.1242/dev.078592/-/DC1

References

Adachi-Yamada, T. and O'Connor, M. B. (2002). Morphogenetic apoptosis: a mechanism for correcting discontinuities in morphogen gradients. *Dev. Biol.* **251**, 74-90.
Adachi-Yamada, T., Fujimura-Kamada, K., Nishida, Y. and Matsumoto, K. (1999). Distortion of proximodistal information causes JNK-dependent apoptosis in Drosophila wing. *Nature* **400**, 166-169.
Andersen, E. D., Krasilnikoff, P. A. and Overvad, H. (1971). Intermittent muscular weakness, extrasystoles, and multiple developmental anomalies. A new syndrome? *Acta Paediatr. Scand.* **60**, 559-564.
Bandyopadhyay, A., Tsuji, K., Cox, K., Harfe, B. D., Rosen, V. and Tabin, C. J. (2006). Genetic analysis of the roles of BMP2, BMP4, and BMP7 in limb patterning and skeletogenesis. *PLoS Genet.* **2**, e216.
Bendahhou, S., Donaldson, M. R., Plaster, N. M., Tristani-Firouzi, M., Fu, Y. H. and Ptácek, L. J. (2003). Defective potassium channel Kir2.1 trafficking underlies Andersen-Tawil syndrome. *J. Biol. Chem.* **278**, 51779-51785.
Bichet, D., Haass, F. A. and Jan, L. Y. (2003). Merging functional studies with structures of inward-rectifier K(+) channels. *Nat. Rev. Neurosci.* **4**, 957-967.
Bjork, B. C., Turbe-Doan, A., Prysak, M., Herron, B. J. and Beier, D. R. (2010). Prdm16 is required for normal palatogenesis in mice. *Hum. Mol. Genet.* **19**, 774-789.
Blair, S. S. (2007). Wing vein patterning in Drosophila and the analysis of intercellular signaling. *Annu. Rev. Cell Dev. Biol.* **23**, 293-319.
Brook, W. J. and Cohen, S. M. (1996). Antagonistic interactions between wingless and decapentaplegic responsible for dorsal-ventral pattern in the Drosophila Leg. *Science* **273**, 1373-1377.
Canún, S., Pérez, N. and Beirana, L. G. (1999). Andersen syndrome autosomal dominant in three generations. *Am. J. Med. Genet.* **85**, 147-156.
Cao, J., Pellock, B. J., White, K. and Raftery, L. A. (2006). A commercial phospho-Smad antibody detects endogenous BMP signaling in *Drosophila* tissues. *Dros. Inf. Serv.* **89**, 131-135.
Casey, L. M., Lan, Y., Cho, E. S., Maltby, K. M., Gridley, T. and Jiang, R. (2006). Jag2-Notch1 signaling regulates oral epithelial differentiation and palate development. *Dev. Dyn.* **235**, 1830-1844.
Choe, S. (2002). Potassium channel structures. *Nat. Rev. Neurosci.* **3**, 115-121.
Cook, O., Biehs, B. and Bier, E. (2004). brinker and optomotor-blind act coordinately to initiate development of the L5 wing vein primordium in Drosophila. *Development* **131**, 2113-2124.
de Celis, J. F. (1997). Expression and function of decapentaplegic and thick veins during the differentiation of the veins in the Drosophila wing. *Development* **124**, 1007-1018.
del Alamo Rodríguez, D., Terriente Felix, J. and Díaz-Benjumea, F. J. (2004). The role of the T-box gene optomotor-blind in patterning the Drosophila wing. *Dev. Biol.* **268**, 481-492.
Derynck, R., Jarrett, J. A., Chen, E. Y., Eaton, D. H., Bell, J. R., Assoian, R. K. and Goeddel, D. V. (1985). Human transforming growth factor-beta complementary DNA sequence and expression in normal and transformed cells. *Nature* **316**, 701-705.
Dietzl, G., Chen, D., Schnorrer, F., Su, K. C., Barinova, Y., Fellner, M., Gasser, B., Kinsey, K., Oppel, S., Scheiblauer, S. et al. (2007). A genome-wide transgenic RNAi library for conditional gene inactivation in Drosophila. *Nature* **448**, 151-156.
Döring, F., Wischmeyer, E., Kühnlein, R. P., Jäckle, H. and Karschin, A. (2002). Inwardly rectifying K+ (Kir) channels in Drosophila. A crucial role of cellular milieu factors Kir channel function. *J. Biol. Chem.* **277**, 25554-25561.

Dudas, M., Sridurongrit, S., Nagy, A., Okazaki, K. and Kaartinen, V. (2004). Craniofacial defects in mice lacking BMP type I receptor Alk2 in neural crest cells. *Mech. Dev.* **121**, 173-182.
Eivers, E., Demagny, H. and De Robertis, E. M. (2009a). Integration of BMP and Wnt signaling via vertebrate Smad1/5/8 and Drosophila Mad. *Cytokine Growth Factor Rev.* **20**, 357-365.
Eivers, E., Fuentealba, L. C., Sander, V., Clemens, J. C., Hartnett, L. and De Robertis, E. M. (2009b). Mad is required for wingless signaling in wing development and segment patterning in Drosophila. *PLoS ONE* **4**, e6543.
Eivers, E., Demagny, H., Choi, R. H. and De Robertis, E. M. (2011). Phosphorylation of Mad controls competition between wingless and BMP signaling. *Sci. Signal.* **4**, ra68.
Ferretti, E., Li, B., Zewdu, R., Wells, V., Hebert, J. M., Karner, C., Anderson, M. J., Williams, T., Dixon, J., Dixon, M. J. et al. (2011). A conserved Pbx-Wnt-p63-Irf6 regulatory module controls face morphogenesis by promoting epithelial apoptosis. *Dev. Cell* **21**, 627-641.
Fujise, M., Takeo, S., Kamimura, K., Matsuo, T., Aigaki, T., Izumi, S. and Nakato, H. (2003). Dally regulates Dpp morphogen gradient formation in the Drosophila wing. *Development* **130**, 1515-1522.
Gelbart, W. M. (1982). Synapsis-dependent allelic complementation at the decapentaplegic gene complex in Drosophila melanogaster. *Proc. Natl. Acad. Sci. USA* **79**, 2636-2640.
Grisaru, S., Cano-Gauci, D., Tee, J., Filmus, J. and Rosenblum, N. D. (2001). Glypican-3 modulates BMP- and FGF-mediated effects during renal branching morphogenesis. *Dev. Biol.* **231**, 31-46.
Gullaud, M., Delanoue, R. and Silber, J. (2003). A Drosophila model to study the functions of TWIST orthologs in apoptosis and proliferation. *Cell Death Differ.* **10**, 641-651.
Halachmi, N., Schulze, K. L., Inbal, A. and Salzberg, A. (2007). Additional sex combs affects antennal development by means of spatially restricted repression of Antp and wg. *Dev. Dyn.* **236**, 2118-2130.
Hatten, M. E., Liem, R. K. and Mason, C. A. (1984). Defects in specific associations between astroglia and neurons occur in microcultures of weaver mouse cerebellar cells. *J. Neurosci.* **4**, 1163-1172.
Hatten, M. E., Liem, R. K. and Mason, C. A. (1986). Weaver mouse cerebellar granule neurons fail to migrate on wild-type astroglial processes in vitro. *J. Neurosci.* **6**, 2676-2683.
Hay, B. A., Wolff, T. and Rubin, G. M. (1994). Expression of baculovirus P35 prevents cell death in Drosophila. *Development* **120**, 2121-2129.
He, F., Xiong, W., Wang, Y., Li, L., Liu, C., Yamagami, T., Taketo, M. M., Zhou, C. and Chen, Y. (2011). Epithelial Wnt/β-catenin signaling regulates palatal shelf fusion through regulation of Tgfβ3 expression. *Dev. Biol.* **350**, 511-519.
Hibino, H., Inanobe, A., Furutani, K., Murakami, S., Findlay, I. and Kurachi, Y. (2010). Inwardly rectifying potassium channels: their structure, function, and physiological roles. *Physiol. Rev.* **90**, 291-366.
Huh, J. R., Guo, M. and Hay, B. A. (2004). Compensatory proliferation induced by cell death in the Drosophila wing disc requires activity of the apical cell death caspase Dronc in a nonapoptotic role. *Curr. Biol.* **14**, 1262-1266.
Irish, V. F. and Gelbart, W. M. (1987). The decapentaplegic gene is required for dorsal-ventral patterning of the Drosophila embryo. *Genes Dev.* **1**, 868-879.
Jackson, S. M., Nakato, H., Sugiura, M., Jannuzi, A., Oakes, R., Kaluza, V., Golden, C. and Selleck, S. B. (1997). dally, a Drosophila glypican, controls cellular responses to the TGF-beta-related morphogen, Dpp. *Development* **124**, 4113-4120.
Jernvall, J., Aberg, T., Kettunen, P., Keränen, S. and Thesleff, I. (1998). The life history of an embryonic signaling center: BMP-4 induces p21 and is associated with apoptosis in the mouse tooth enamel knot. *Development* **125**, 161-169.
Jiang, R., Lan, Y., Chapman, H. D., Shawber, C., Norton, C. R., Serreze, D. V., Weinmaster, G. and Gridley, T. (1998). Defects in limb, craniofacial, and thymic development in Jagged2 mutant mice. *Genes Dev.* **12**, 1046-1057.
Jin, Y. R., Turcotte, T. J., Crocker, A. L., Han, X. H. and Yoon, J. K. (2011). The canonical Wnt signaling activator, R-spondin2, regulates craniofacial patterning and morphogenesis within the branchial arch through ectodermal-mesenchymal interaction. *Dev. Biol.* **352**, 1-13.
Kim, J., Johnson, K., Chen, H. J., Carroll, S. and Laughon, A. (1997). Drosophila Mad binds to DNA and directly mediates activation of vestigial by Decapentaplegic. *Nature* **388**, 304-308.
Lécuyer, E., Parthasarathy, N. and Krause, H. M. (2008). Fluorescent in situ hybridization protocols in Drosophila embryos and tissues. *Methods Mol. Biol.* **420**, 289-302.
Letsou, A., Arora, K., Wrana, J. L., Simin, K., Twombly, V., Jamal, J., Staehling-Hampton, K., Hoffmann, F. M., Gelbart, W. M., Massagué, J. et al. (1995). Drosophila Dpp signaling is mediated by the punt gene product: a dual ligand-binding type II receptor of the TGF beta receptor family. *Cell* **80**, 899-908.
Lin, C., Fisher, A. V., Yin, Y., Maruyama, T., Veith, G. M., Dhandha, M., Huang, G. J., Hsu, W. and Ma, L. (2011). The inductive role of Wnt-β-Catenin signaling in the formation of oral apparatus. *Dev. Biol.* **356**, 40-50.
Liu, W., Selever, J., Murali, D., Sun, X., Brugger, S. M., Ma, L., Schwartz, R. J., Maxson, R., Furuta, Y. and Martin, J. F. (2005). Threshold-specific requirements for Bmp4 in mandibular development. *Dev. Biol.* **283**, 282-293.
Livak, K. J. and Schmittgen, T. D. (2001). Analysis of relative gene expression data using real-time quantitative PCR and the 2(–Delta Delta C(T)) Method. *Methods* **25**, 402-408.
Lu, R., Niesen, M. J., Hu, W., Vaidehi, N. and Shively, J. E. (2011). Interaction of actin with carcinoembryonic antigen-related cell adhesion molecule 1 (CEACAM1) receptor in liposomes is Ca2+- and phospholipid-dependent. *J. Biol. Chem.* **286**, 27528-27536.
MacLean, S. J., Andrews, B. C. and Verheyen, E. M. (2002). Characterization of Dir: a putative potassium inward rectifying channel in Drosophila. *Mech. Dev.* **116**, 193-197.
Marquez, R. M., Singer, M. A., Takaesu, N. T., Waldrip, W. R., Kraytsberg, Y. and Newfeld, S. J. (2001). Transgenic analysis of the Smad family of TGF-beta signal transducers in Drosophila melanogaster suggests new roles and new interactions between family members. *Genetics* **157**, 1639-1648.
Martín, F. A., Pérez-Garijo, A., Moreno, E. and Morata, G. (2004). The brinker gradient controls wing growth in Drosophila. *Development* **131**, 4921-4930.
Mason, A. J., Hayflick, J. S., Ling, N., Esch, F., Ueno, N., Ying, S. Y. and Seeburg, P. H. (1985). Complementary DNA sequences of ovarian follicular fluid inhibin show precursor structure and homology with transforming growth factor-beta. *Nature* **318**, 659-663.
McLerie, M. and Lopatin, A. N. (2003). Dominant-negative suppression of I(K1) in the mouse heart leads to altered cardiac excitability. *J. Mol. Cell. Cardiol.* **35**, 367-378.
Menezes, R., Letra, A., Kim, A. H., Küchler, E. C., Day, A., Tannure, P. N., Gomes da Motta, L., Paiva, K. B., Granjeiro, J. M. and Vieira, A. R. (2010). Studies with Wnt genes and nonsyndromic cleft lip and palate. *Birth Defects Res. A Clin. Mol. Teratol.* **88**, 995-1000.
Moreno, E., Basler, K. and Morata, G. (2002). Cells compete for decapentaplegic survival factor to prevent apoptosis in Drosophila wing development. *Nature* **416**, 755-759.
Nellen, D., Affolter, M. and Basler, K. (1994). Receptor serine/threonine kinases implicated in the control of Drosophila body pattern by decapentaplegic. *Cell* **78**, 225-237.
Neubüser, A., Peters, H., Balling, R. and Martin, G. R. (1997). Antagonistic interactions between FGF and BMP signaling pathways: a mechanism for positioning the sites of tooth formation. *Cell* **90**, 247-255.
O'Connor, M. B., Umulis, D., Othmer, H. G. and Blair, S. S. (2006). Shaping BMP morphogen gradients in the Drosophila embryo and pupal wing. *Development* **133**, 183-193.
Ohta, M., Greenberger, J. S., Anklesaria, P., Bassols, A. and Massague, J. (1987). Two forms of transforming growth factor-beta distinguished by multipotential haematopoietic progenitor cells. *Nature* **329**, 539-541.
Padgett, R. W., St Johnston, R. D. and Gelbart, W. M. (1987). A transcript from a Drosophila pattern gene predicts a protein homologous to the transforming growth factor-beta family. *Nature* **325**, 81-84.
Paine-Saunders, S., Viviano, B. L., Economides, A. N. and Saunders, S. (2002). Heparan sulfate proteoglycans retain Noggin at the cell surface: a potential mechanism for shaping bone morphogenetic protein gradients. *J. Biol. Chem.* **277**, 2089-2096.
Parks, A. L., Cook, K. R., Belvin, M., Dompe, N. A., Fawcett, R., Huppert, K., Tan, L. R., Winter, C. G., Bogart, K. P., Deal, J. E. et al. (2004). Systematic generation of high-resolution deletion coverage of the Drosophila melanogaster genome. *Nat. Genet.* **36**, 288-292.
Patil, N., Cox, D. R., Bhat, D., Faham, M., Myers, R. M. and Peterson, A. S. (1995). A potassium channel mutation in weaver mice implicates membrane excitability in granule cell differentiation. *Nat. Genet.* **11**, 126-129.
Pérez-Garijo, A., Martín, F. A. and Morata, G. (2004). Caspase inhibition during apoptosis causes abnormal signalling and developmental aberrations in Drosophila. *Development* **131**, 5591-5598.
Pérez-Garijo, A., Martín, F. A., Struhl, G. and Morata, G. (2005). Dpp signaling and the induction of neoplastic tumors by caspase-inhibited apoptotic cells in Drosophila. *Proc. Natl. Acad. Sci. USA* **102**, 17664-17669.
Peters, H., Neubüser, A., Kratochwil, K. and Balling, R. (1998). Pax9-deficient mice lack pharyngeal pouch derivatives and teeth and exhibit craniofacial and limb abnormalities. *Genes Dev.* **12**, 2735-2747.
Rakic, P. and Sidman, R. L. (1973). Weaver mutant mouse cerebellum: defective neuronal migration secondary to abnormality of Bergmann glia. *Proc. Natl. Acad. Sci. USA* **70**, 240-244.
Richardson, R. J., Dixon, J., Jiang, R. and Dixon, M. J. (2009). Integration of IRF6 and Jagged2 signalling is essential for controlling palatal adhesion and fusion competence. *Hum. Mol. Genet.* **18**, 2632-2642.
Ruberte, E., Marty, T., Nellen, D., Affolter, M. and Basler, K. (1995). An absolute requirement for both the type II and type I receptors, punt and thick veins, for dpp signaling in vivo. *Cell* **80**, 889-897.
Ryoo, H. D., Gorenc, T. and Steller, H. (2004). Apoptotic cells can induce compensatory cell proliferation through the JNK and the Wingless signaling pathways. *Dev. Cell* **7**, 491-501.

Sampath, T. K., Rashka, K. E., Doctor, J. S., Tucker, R. F. and Hoffmann, F. M. (1993). Drosophila transforming growth factor beta superfamily proteins induce endochondral bone formation in mammals. *Proc. Natl. Acad. Sci. USA* **90**, 6004-6008.

Sanford, L. P., Ormsby, I., Gittenberger-de Groot, A. C., Sariola, H., Friedman, R., Boivin, G. P., Cardell, E. L. and Doetschman, T. (1997). TGFbeta2 knockout mice have multiple developmental defects that are non-overlapping with other TGFbeta knockout phenotypes. *Development* **124**, 2659-2670.

Sansone, V., Griggs, R. C., Meola, G., Ptácek, L. J., Barohn, R., Iannaccone, S., Bryan, W., Baker, N., Janas, S. J., Scott, W. et al. (1997). Andersen's syndrome: a distinct periodic paralysis. *Ann. Neurol.* **42**, 305-312.

Schaller, S. A. and Muneoka, K. (2001). Inhibition of polarizing activity in the anterior limb bud is regulated by extracellular factors. *Dev. Biol.* **240**, 443-456.

Schaller, S. A., Li, S., Ngo-Muller, V., Han, M. J., Omi, M., Anderson, R. and Muneoka, K. (2001). Cell biology of limb patterning. *Int. Rev. Cytol.* **203**, 483-517.

Segal, D. and Gelbart, W. M. (1985). Shortvein, a new component of the decapentaplegic gene complex in Drosophila melanogaster. *Genetics* **109**, 119-143.

Signorini, S., Liao, Y. J., Duncan, S. A., Jan, L. Y. and Stoffel, M. (1997). Normal cerebellar development but susceptibility to seizures in mice lacking G protein-coupled, inwardly rectifying K+ channel GIRK2. *Proc. Natl. Acad. Sci. USA* **94**, 923-927.

Silverman, S. K., Kofuji, P., Dougherty, D. A., Davidson, N. and Lester, H. A. (1996). A regenerative link in the ionic fluxes through the weaver potassium channel underlies the pathophysiology of the mutation. *Proc. Natl. Acad. Sci. USA* **93**, 15429-15434.

Skeath, J. B. and Carroll, S. B. (1991). Regulation of achaete-scute gene expression and sensory organ pattern formation in the Drosophila wing. *Genes Dev.* **5**, 984-995.

Spencer, F. A., Hoffmann, F. M. and Gelbart, W. M. (1982). Decapentaplegic: a gene complex affecting morphogenesis in Drosophila melanogaster. *Cell* **28**, 451-461.

Tabata, T. and Kornberg, T. B. (1994). Hedgehog is a signaling protein with a key role in patterning Drosophila imaginal discs. *Cell* **76**, 89-102.

Tawil, R., Ptacek, L. J., Pavlakis, S. G., DeVivo, D. C., Penn, A. S., Ozdemir, C. and Griggs, R. C. (1994). Andersen's syndrome: potassium-sensitive periodic paralysis, ventricular ectopy, and dysmorphic features. *Ann. Neurol.* **35**, 326-330.

Taya, Y., O'Kane, S. and Ferguson, M. W. (1999). Pathogenesis of cleft palate in TGF-beta3 knockout mice. *Development* **126**, 3869-3879.

Teleman, A. A. and Cohen, S. M. (2000). Dpp gradient formation in the Drosophila wing imaginal disc. *Cell* **103**, 971-980.

Tong, Y., Wei, J., Zhang, S., Strong, J. A., Dlouhy, S. R., Hodes, M. E., Ghetti, B. and Yu, L. (1996). The weaver mutation changes the ion selectivity of the affected inwardly rectifying potassium channel GIRK2. *FEBS Lett.* **390**, 63-68.

Tucker, A. S., Al Khamis, A. and Sharpe, P. T. (1998a). Interactions between Bmp-4 and Msx-1 act to restrict gene expression to odontogenic mesenchyme. *Dev. Dyn.* **212**, 533-539.

Tucker, A. S., Matthews, K. L. and Sharpe, P. T. (1998b). Transformation of tooth type induced by inhibition of BMP signaling. *Science* **282**, 1136-1138.

Xu, J., Krebs, L. T. and Gridley, T. (2010). Generation of mice with a conditional null allele of the Jagged2 gene. *Genesis* **48**, 390-393.

Yapici, N., Kim, Y. J., Ribeiro, C. and Dickson, B. J. (2008). A receptor that mediates the post-mating switch in Drosophila reproductive behaviour. *Nature* **451**, 33-37.

Yoon, G., Oberoi, S., Tristani-Firouzi, M., Etheridge, S. P., Quitania, L., Kramer, J. H., Miller, B. L., Fu, Y. H. and Ptáček, L. J. (2006a). Andersen-Tawil syndrome: prospective cohort analysis and expansion of the phenotype. *Am. J. Med. Genet.* **140A**, 312-321.

Yoon, G., Quitania, L., Kramer, J. H., Fu, Y. H., Miller, B. L. and Ptácek, L. J. (2006b). Andersen-Tawil syndrome: definition of a neurocognitive phenotype. *Neurology* **66**, 1703-1710.

Zaritsky, J. J., Eckman, D. M., Wellman, G. C., Nelson, M. T. and Schwarz, T. L. (2000). Targeted disruption of Kir2.1 and Kir2.2 genes reveals the essential role of the inwardly rectifying K(+) current in K(+)-mediated vasodilation. *Circ. Res.* **87**, 160-166.

Zecca, M., Basler, K. and Struhl, G. (1995). Sequential organizing activities of engrailed, hedgehog and decapentaplegic in the Drosophila wing. *Development* **121**, 2265-2278.

Ziv, O., Suissa, Y., Neuman, H., Dinur, T., Geuking, P., Rhiner, C., Portela, M., Lolo, F., Moreno, E. and Gerlitz, O. (2009). The co-regulator dNAB interacts with Brinker to eliminate cells with reduced Dpp signaling. *Development* **136**, 1137-1145.

Zuzarte-Luis, V. and Hurle, J. M. (2005). Programmed cell death in the embryonic vertebrate limb. *Semin. Cell Dev. Biol.* **16**, 261-269.